Polyhedron 85 (2015) 511–518

Contents lists available at ScienceDirect

Polyhedron

journal homepage: www.elsevier.com/locate/poly

Synthesis, characterization, spectroscopic and electrochemical studies of donor–acceptor ruthenium(II) polypyridine ligand derivatives with potential NLO applications

César Zúñiga [a], Irma Crivelli [b], Bárbara Loeb [a,*]

[a] Facultad de Química, Pontificia Universidad Católica de Chile, Casilla 306, Santiago, Chile
[b] Facultad de Ciencias, Universidad de Chile, Las Palmeras 3425, Santiago, Chile

ARTICLE INFO

Article history:
Received 18 March 2014
Accepted 8 September 2014
Available online 28 September 2014

Keywords:
Ruthenium complexes
Solvatochromic effect
MLCT
NLO
Donor-Acceptor effect

ABSTRACT

In this work we report the preparation of six new donor–metal–acceptor (D–M–A) type complexes of ruthenium(II) with the highly absorbing "chromophoric" ligand 4,4′-bis(2-(4-methoxyphenyl)styryl)-2,2′-bipyridine, (L-OCH_3, donor moiety) and substituted polypyridinic ligands with electron acceptor character (NN-A). The NN-A studied ligands were pyrazino[2,3-f][1,10]phenanthroline (ppl), 11-R-dipyrido[2,3-a:2′,3′-c]phenazine (dppz-R; R is H, NO_2, or CN) and 10,11-[1,4-naphtalenedione]dipyrido[3,2-a:2′,3′-c]phenazine (Aqphen). The complexes were characterized by IR, NMR, UV–Vis spectroscopy and cyclic voltammetry. The potential NLO response of the complexes was evaluated by solvatochromic studies. Although the communication between D and A exists, the effect of the change of the acceptor moiety on the properties of the complexes is small and the behavior of the complexes is governed mainly by the donor ligand. The Metal to Ligand Charge Transfer bands (MLCT) exhibited by all complexes in the visible region have dominant electronic density transfer character from the metal to the chromophoric L-OCH_3 ligand. The hypsochromic shift of this low energy absorption band on going from a less polar (benzene) to a more polar solvent (acetonitrile) indicated that a redistribution of the electronic density among the metal and the donor ligand is observed. This behavior permits to predict a NLO response for these types of complexes. The combination of high molar absorptivity with intraligand charge transfer (ILCT) mixing into the MLCT bands are encouraging for the generation of new materials with interesting NLO properties.

1. Introduction

The nonlinear optical (NLO) properties of various classes of metal complexes have been systematically explored in the search for new and optimized NLO materials. Both early [1–4] and more recent [5–10] review articles of metal complexes indicate the breadth of the active research in this field, with the majority of studies focusing on quadratic nonlinearities in complexes with a donor(D)–bridge–acceptor(A) composition. The introduction of an organometallic fragment offers further possibilities for modification and tuning of the electronic and/or optical properties of these materials. Connection of the metal in an electron donor or acceptor group to another acceptor or donor group, either directly or via a conjugated π-network, leads to intense and low-energy intramolecular charge transfer (ICT) transitions [11]. The NLO activity of this class of compounds depends not only on the strength of the D–A pair but also on the nature of the π-conjugated spacer [12–15]. Materials expected to generate high non-linear optical responses should fulfil the following conditions: (i) a low energy CT transition related to a small Δ(HOMO–LUMO) which can immediately be derived from UV–Vis spectra; (ii) a large transition dipole moment related to the oscillator strength, which can be calculated from the integrated intensity of the CT band; (iii) a large change in the dipole moment $\Delta\mu eg$ [16]. In this context, a number of NLO dipolar and octupolar metal complexes, mainly based on bipyridine ligands, have been reported in the literature and recently reviewed [17,18]. Complexes of ruthenium(II) with polypyridine ligands displayed a low energy Metal to Ligand Charge Transfer (MLCT) bands with good molar extinction coefficients (ε) due to electron delocalization [19–21], which changed the electric dipole moment associated with the charge-transfer (CT) state as indicated by the solvatochromic effect on this band [16].

In this work we report the preparation, characterization and the evaluation of potential NLO response of new metallic complexes of ruthenium(II) with the highly absorbing "chromophoric" ligand

* Corresponding author.
E-mail address: bloeb@puc.cl (B. Loeb).

http://dx.doi.org/10.1016/j.poly.2014.09.004
0277-5387/

4,4′-bis(2-(4-methoxyphenyl)styryl)-2,2′-bipyridine, (*L-OCH$_3$*, donor moiety) and substituted polypyridinic ligands with electron acceptor character (NN-A, acceptor group) such as pyrazino[2,3-f][1,10]phenanthroline (ppl), 11-R-dipyrido[2,3-a:2′,3′-c]phenazine (dppz-R; R: H, NO_2, CN) and 10,11-[1,4-naphtalenedione]dipyrido[3,2-a:2′,3′-c]phenazine (Aqphen):

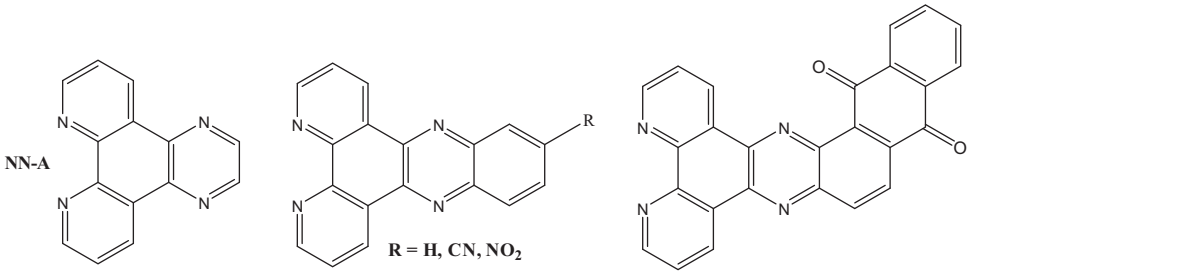

Based on the solvatochromic effect observed, a potential NLO response is anticipated.

2. Experimental

2.1. General methods and materials

Organic solvents were purified by standard methods. All chemicals were reagent-grade, purchased from Aldrich and used as received unless otherwise specified. 4,4′-Bis(2-(4-methoxyphenyl)ethyl)-2,2′-bipyridine [L-OCH_3] was prepared by a modification of the synthesis reported in the literature [22] that will be described in Section 2.3, and the precursor complex, *cis*-[Ru(L-OCH_3)$_2$Cl$_2$], was prepared according to a literature procedure [23].

IR spectra were obtained using a Bruker VECTOR 22 FT-IR spectrophotometer in solid mode (KBr cell, 0.2 mm in length). ^{1}H NMR and ^{1}H–^{1}H COSY spectra were obtained on a Bruker AVANCE 400 spectrometer, all spectra being referred to TMS as an internal standard. UV–Vis absorption spectra were recorded on a Shimadzu UV–Vis–NIR 3101 PC160 instrument using 1-cm quartz cells. Electrochemistry measurements (cyclic voltammetry) were carried out with a BAS CV-50 W unit. A conventional three-electrode configuration was used, consisting of a platinum working electrode, a platinum wire as the auxiliary electrode, and Ag/$AgNO_3$ as the reference electrode. All solutions were prepared in acetonitrile, freshly distilled over P_4O_{10} with 0.1 M TBAH (tetrabutylammonium hexafluorophosphate) as the supporting electrolyte, and thoroughly degassed with N_2 prior to each experiment. Cyclic voltammograms were run at a sweep rate of 100 mV s^{-1}. The reported $E_{½}$ values were calculated as the semidifference between the E_p corresponding to the cathodic and anodic waves: $E_{½} = (E_c + E_a)/2$. Elemental analyses were performed using a CE Instruments model EA 1108 elemental analyser.

2.2. Synthesis of 4,4′-bis(2-hydroxy-2-(4-methoxyphenyl)styryl)-2,2′-bipyridine

The synthetic method was adapted from the synthesis of an analogous compound [23]. 0.50 g (2.71 mmol) of 4,4′-Dimethyl-2,2′-dipyridyl was dissolved in 20 mL of dry tetrahydrofuran (THF) at 0 °C, under nitrogen, and added dropwise to a solution of diisopropylamine (3.5 mL, 24.9 mmol). The mixture was stirred at 0 °C for 75 min; then a solution of 4-Methoxybenzaldehyde 0.66 mL (5.42 mmol) in 10 mL of dry THF was added over a 5 min period. The mixture was stirred at 0 °C for 5 h and then at room temperature for 16 h. Then it was quenched with 2 mL of methanol and 18 mL of water, whereupon the color changed from orange to a light yellow. The product was extracted with CH_2Cl_2 (3 × 30 mL). The organic phase was dried over anhydrous Na_2SO_4 and the solvent was evaporated to give the product. The solid was washed three times with diethyl ether and was filtered and dried under vacuum.

Yield: 56%. IR (cm^{-1}): 3385 *ν*(O—H); 3061 *ν*(CH aromatic); 2835 *ν*(CH aliphatic); 1598 *ν*(C=N); 1249 *ν*(C—O—C asymmetric); 1033 *ν*(C—O—C symmetric). ^{1}H NMR ($CDCl_3$, 400 MHz, *δ* ppm): 3.07 (m, 4H, Hx); 3.79 (s, 6H, OCH_3); 4.27 (m 1H′); 6.86 (d, *J* = 8.8 Hz, 4H, H_9); 7.08 (d, *J* = 5.0 Hz, 2H, H_5); 7.28 (d, *J* = 8.8 Hz, 4H, H_8); 8.26 (s, 2H, H_3); 8.50 (d, *J* = 5.1 Hz, 2H, H_6).

2.3. Synthesis of 4,4′-bis(2-(4-methoxyphenyl)styryl)-2,2′-bipyridine [L-OCH_3]

1.0 g (2.10 mmol) of 4,4′-bis(2-hydroxy-2-(4-methoxyphenyl)styryl)-2,2′-bipyridine was dissolved in 50 mL of 10% aqueous H_2SO_4 solution; the mixture was heated at 90 °C for 2 h and then cooled in an ice bath and neutralized with 1 M aqueous NaOH to yield a light yellow precipitate. The product was filtered, washed with water, then acetone and dried under vacuum, giving L-OCH_3 as a yellow solid. The numbering of hydrogen atoms is shown in Fig. 1 in order to follow the assignment of the ^{1}H NMR signals of the L-OCH_3 ligand.

Yield: 73%. *Anal.* Calc. for $C_{28}H_{24}N_2O_2$: C, 79.98; H, 5.75; N, 6.66. Found: C, 80.59; H, 5.80; N, 6.79%. IR (cm^{-1}): 3027 *ν*(CH aromatic); 2833 *ν*(CH aliphatic); 1580 *ν*(C= N); 1249 *ν*(C—O—C asymmetric); 1028 *ν*(C—O—C symmetric). ^{1}H NMR ($CDCl_3$, 400 MHz, *δ* ppm): 3.85 (s, 6H, OCH_3); 6.94 (d, *J* = 8.7 Hz, 4H, H_9); 7.00 (d, *J* = 16.3 Hz,

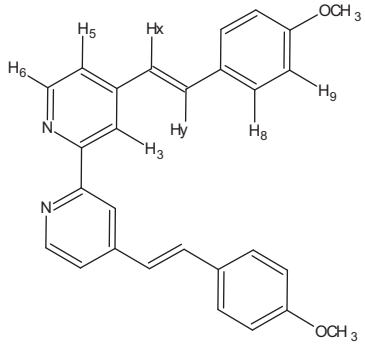

Fig. 1. Proton numbering for the ^{1}H NMR signals of the L-OCH_3 ligand.

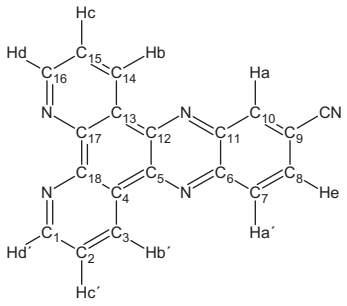

Fig. 2. Proton and carbon numbering for the NMR signals of the dppz-CN ligand.

2H, Hx); 7.37 (dd, J = 5.1 Hz/1.2 Hz, 2H, H_5); 7.42 (d, J = 16.3 Hz, 2H, Hy); 7.52 (d, J = 8.7 Hz, 4H, H_8); 8.52 (s, 2H, H_3); 8.65 (d, J = 5.1 Hz, 2H, H_6).

2.4. Synthesis of 11-cyanodipyrido[2,3-a:2′,3′-c]phenazine (dppz-CN)

1.00 g (4.80 mmol) of 1,10-phenanthroline-5,6-dione and 0.64 g (4.80 mmol) of 3,4-diaminobenzonitrile were dissolved in 80 mL of methanol and the mixture was refluxed for 5 h. The mixture was allowed to cool and the resultant precipitate filtered and washed with MeOH and diethyl ether to give a light red solid that was dried in vacuum. The numbering of hydrogen atoms is shown in Fig. 2 in order to follow the assignment of the ^{1}H NMR signals of the dppz-CN ligand.

Yield: 86%. *Anal.* Calc. for $C_{19}H_9N_5$: C, 74.27; H, 2.94; N, 22.79. Found: C, 74.26; H, 2.94; N, 22.84%. IR (cm^{-1}): 3060 ν(CH aromatic); 2227 ν(C≡N); 1584 ν(C=N). ^{1}H NMR ($CDCl_3$, 400 MHz, δ ppm): 7.68–7.73 (m, 2H, Hc y Hc′); 7.95 (dd, J = 1.7 Hz/8.8 Hz, 1H, Ha′); 8.29 (d, J = 8.8 Hz, 1H, He); 8.57 (d, J = 1.3 Hz, 1H, Ha); 9.22–9.25 (m, 2H, Hd and Hd′); 9.35–9.42 (m, 2H, Hb and Hb′). ^{13}C {^{1}H} NMR ($CDCl_3$, δ ppm): 123.5 (C_2); 123.6 (C_{15}); 129.9 (C_7); 130.4 (C_8); 133.1 (C_3); 133.3 (C_{14}); 134.9 (C_{10}); 152.6 (C_1); 152.8 (C_{16}).

2.5. Synthesis of Tris(4,4′-bis(2-(4-methoxyphenyl)styryl)-2,2′-bipyridine)ruthenium bis(hexafluorophosphate) [Ru(L-OCH_3)$_3$](PF_6)$_2$ (**1**)

54 mg (0.26 mmol) $RuCl_3{\cdot}3H_2O$ and 330 mg (0.78 mmol) of L-OCH_3 were stirred at reflux in 40 mL EtOH/H_2O (1:1) under nitrogen atmosphere for 24 h. The ethanol was removed by rotary evaporation and a solution of 254 mg (1.56 mmol) NH_4PF_6 in water (10 mL) was added, after which a deep-red precipitate appeared, as depicted in Scheme 1. The solid was filtered off, washed with water and diethyl ether. The crude product was purified by chromatography in aluminum oxide prepared with CH_3Cl, and the desired compounds were eluted with acetone. The deep red-wine band was collected and the solvent removed by rotary evaporation, the solid was then dissolved in a minimum volume of acetone, and the solid precipitated with ethyl ether.

Yield: 24%. *Anal.* Calc. for $RuC_{84}H_{72}N_6O_6P_2F_{12}$: C, 61.05; H, 4.39; N, 5.09. Found: C, 61.68; H, 4.45; N, 5.12%. IR (cm^{-1}): 3028 ν(CH aromatic); 2836 ν(CH aliphatic); 1596 ν(C=N); 1252 ν(C—O—C asymmetric); 1028 ν(C—O—C symmetric); 842 and 557 ν(P—F_6). ^{1}H NMR (acetone-d_6, 400 MHz, δ ppm): 3.84 (s, 18H, OCH_3); 7.00 (d, J = 8.4 Hz, 12H, H_9); 7.30 (d, J = 16.5 Hz, 6H, Hy); 7.66 (d, J = 9.1 Hz, 18H, H_8, and H_5,); 7.76 (d, J = 16.1 Hz, 6H, Hx); 8.02 (t, 6H, H_6); 9.00 (s, 6H, H_3).

2.6. General procedure for the synthesis of heteroleptic ruthenium complexes

150 mg (0.148 mmol) *cis*-Ru(L-OCH_3)$_2$$Cl_2$, silver hexafluorophosphate 75 mg (0.296 mmol) and 0.148 mmol of the appropriate polypyridinic ligand were dissolved in 50 mL of dimethylformamide (DMF). The resulting solution was then refluxed and stirred for 8 h under nitrogen atmosphere, during which the solution changed to a deep red-wine color. After cooling, the reaction mixture was

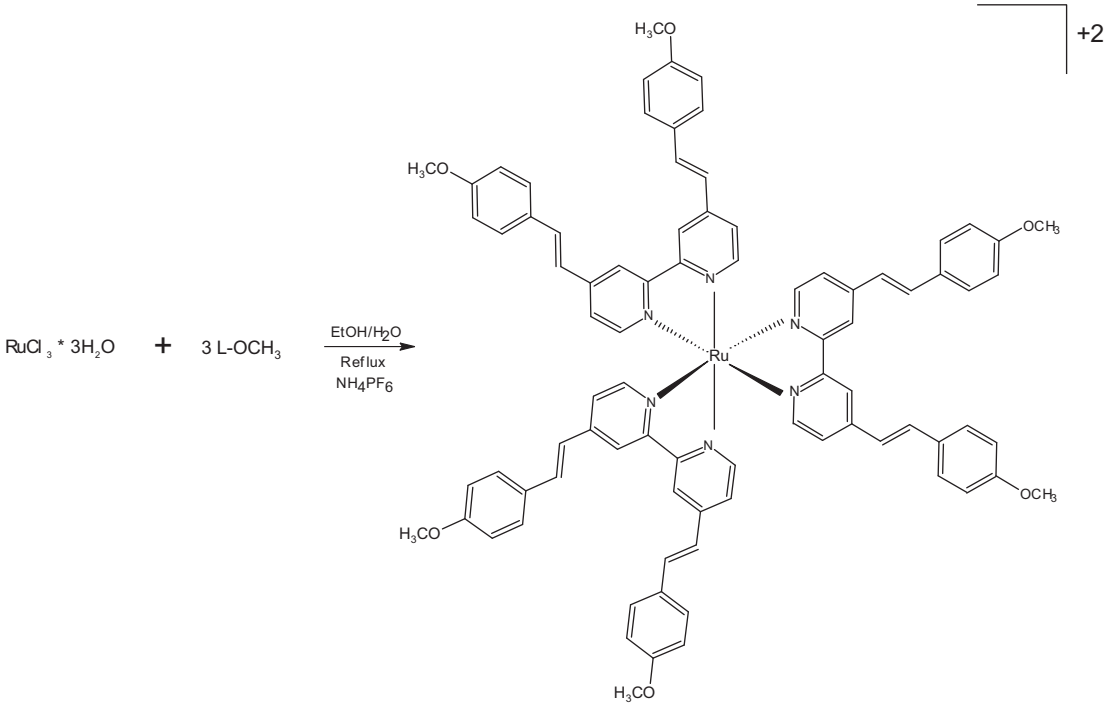

Scheme 1. Synthesis of Tris(4,4′-bis(2-(4-methoxyphenyl)styryl)-2,2′-bipyridine)ruthenium bis(hexafluorophosphate). The numbering of hydrogen atoms is shown in Fig. 1 in order to follow the assignment of the ^{1}H NMR signals of the L-OCH_3 ligand.

filtered through a pad of Celite. The solvent of the deep red-wine solution was removed by rotary evaporation and the crude product was then dissolved in a minimal amount of acetone. A saturated aqueous ammonium hexafluorophosphate solution was added and the precipitate collected and washed with diethyl ether. The crude product was filtered off and purified by chromatography in aluminum oxide in the same way as described in Section 2.5.

*2.6.1. [Ru(L-OCH$_3$)$_2$ppl](PF$_6$)$_2$ (**2**)*

Yield: 44%. *Anal.* Calc. for $RuC_{70}H_{56}N_8O_4P_2F_{12}$ (+1.0 acetone): C, 57.60; H, 4.10; N, 7.36. Found: C, 56.40; H, 4.05; N, 7.35%. IR (cm^{-1}): 3072 *ν*(CH aromatic); 2837 *ν*(CH aliphatic); 1596 *ν*(C═N); 1253 *ν*(C—O—C asymmetric); 1027 *ν*(C—O—C symmetric); 840 and 557 *ν*(P—F$_6$). ^{1}H NMR (acetone-*d*$_6$, 400 MHz, *δ* ppm): 3.85 (s, 12H, OCH$_3$); 6.99 (d, *J* = 8.7 Hz, 4H, H$_{9'}$); 7.02 (d, *J* = 8.7 Hz, 4H, H$_9$); 7.24 (d, *J* = 16.1 Hz, 2H, Hy′); 7.33 (d, *J* = 16.5 Hz, 2H, Hy); 7.47 (d, *J* = 5.5 Hz, 2H, H$_{5'}$); 7.62 (d, *J* = 8.7 Hz, 4H, H$_{8'}$); 7.67 (d, *J* = 8.7 Hz, 4H, H$_8$); 7.70 (d, *J* = 16.8 Hz, 2H, Hx′); 7.76 (d, *J* = 5.8 Hz, 2H, H$_5$); 7.79 (d, *J* = 16.5 Hz, 2H, Hx); 7.89 (d, *J* = 6.2 Hz, 2H, H$_{6'}$); 8.13 (dd, *J* = 5.1 Hz/8.4 Hz, 2H, Hc); 8.15 (d, *J* = 6.2 Hz, 2H, H$_6$); 8.71 (d, *J* = 5.1 Hz, 2H, Hd); 9.02 (s, 2H, H$_{3'}$); 9.06 (s, 2H, H$_3$); 9.36 (s, 2H, Ha); 9.66 (d, *J* = 8.1 Hz, 2H, Hb).

*2.6.2. [Ru(L-OCH$_3$)$_2$dppz](PF$_6$)$_2$ (**3**)*

Yield: 23%. *Anal.* Calc. for $RuC_{74}H_{58}N_8O_4P_2F_{12}$ (+0.2 acetone): C, 58.72; H, 3.91; N, 7.34. Found: C, 58.86; H, 3.92; N, 7.35%. IR (cm^{-1}): 3031 *ν*(CH aromatic); 2837 *ν*(CH aliphatic); 1596 *ν*(C═N); 1253 *ν*(C—O—C asymmetric); 1027 *ν*(C—O—C symmetric); 842 and 557 *ν*(P—F$_6$). ^{1}H NMR (acetone-*d*$_6$, 400 MHz, *δ* ppm): 3.84 (d, 12H, OCH$_3$); 6.97 (d, *J* = 8.8 Hz, 4H, H$_{9'}$); 7.00 (d, *J* = 8.6 Hz, 4H, H$_9$); 7.23 (d, *J* = 16.3 Hz, 2H, Hy′); 7.32 (d, *J* = 16.0 Hz, 2H, Hy); 7.51 (d, *J* = 5.6 Hz, 2H, H$_{5'}$); 7.61 (d, *J* = 8.8 Hz, 4H, H$_{8'}$); 7.65 (d, *J* = 7.7 Hz, 4H, H$_8$); 7.69 (d, *J* = 5.6 Hz, 2H, H$_5$); 7.73 (d, *J* = 16.0 Hz, 2H, Hx′); 7.81 (d, *J* = 16.0 Hz, 2H, Hx); 7.97 (d, *J* = 5.9 Hz, 2H, H$_{6'}$); 8.02 (d, *J* = 6.0 Hz, 2H, H$_6$); 8.13 (t, 2H, Hc); 8.18 (d, *J* = 9.5 Hz, 2H, He); 8.46 (d, *J* = 9.6 Hz, 2H, Ha); 8.67 (d, *J* = 5.0 Hz, 2H, Hd); 9.06 (s, 2H, H$_{3'}$); 9.09 (s, 2H, H$_3$); 9.74 (d, *J* = 7.9 Hz, 2H, Hb).

*2.6.3. [Ru(L-OCH$_3$)$_2$dppz-CN](PF$_6$)$_2$ (**4**)*

Yield: 51%. *Anal.* Calc. for $RuC_{75}H_{57}N_9O_4P_2F_{12}$ (+0.6 acetone): C, 58.60; H, 3.88; N, 8.01. Found: C, 57.74; H, 3.83; N, 7.98%. IR (cm^{-1}): 3072 *ν*(CH aromatic); 2837 *ν*(CH aliphatic); 2229 *ν*(C≡N); 1596 *ν*(C═ N); 1253 *ν*(C—O—C asymmetric); 1027 *ν*(C—O—C symmetric); 842 and 557 *ν*(P—F$_6$). ^{1}H NMR (acetone-*d*$_6$, 400 MHz, *δ* ppm): 3.84 (d, 12H, OCH$_3$); 6.67 (d, *J* = 9.0 Hz, 4H, H$_{9'}$); 7.01 (d, *J* = 8.9 Hz, 4H, H$_9$); 7.24 (d, *J* = 16.5 Hz, 2H, Hy′); 7.33 (d, *J* = 16.2 Hz, 2H, Hy); 7.51 (d, *J* = 6.0 Hz, 2H, H$_{5'}$); 7.61 (d, *J* = 8.7 Hz, 4H, H$_{8'}$); 7.66 (d, *J* = 8.7 Hz, 4H, H$_8$); 7.70 (d, *J* = 16.5 Hz, 2H, Hx′); 7.75 (d, *J* = 10.2 Hz, 2H, H$_5$); 7.78 (d, *J* = 16.4 Hz, 2H, Hx); 7.97 (d, *J* = 6.0 Hz, 2H, H$_{6'}$); 8.03 (d, *J* = 6.0 Hz, 1H, Ha); 8.15 (d, *J* = 5.9 Hz, 2H, H$_6$); 8.17 (dd, *J* = 2.5 Hz/6.0 Hz, 2H, Hc, Hc′); 8.37 (dd, *J* = 1.7 Hz/8.8 Hz, 1H, Ha′); 8.66 (d, *J* = 8.9 Hz, 1H, He); 8.73 (d, *J* = 5.5 Hz, 2H, Hd, Hd′); 9.02 (s, 2H, H$_{3'}$); 9.04 (s, 2H, H$_3$); 9.76 (t, 2H, Hb, Hb′).

*2.6.4. [Ru(L-OCH$_3$)$_2$dppz-NO$_2$](PF$_6$)$_2$ (**5**)*

Yield: 40%. *Anal.* Calc. for $RuC_{74}H_{57}N_9O_6P_2F_{12}$ (+0.5 acetone): C, 57.09; H, 3.81; N, 7.94. Found: C, 56.47; H, 3.77; N, 7.93%. IR (cm^{-1}): 3072 *ν*(CH aromatic); 2837 *ν*(CH aliphatic); 1596 *ν*(C═ N); 1511 and 1347 *ν*(NO$_2$); 1253 *ν*(C—O—C asymmetric); 1027 *ν*(C—O—C symmetric); 842 and 557 *ν*(P—F$_6$). ^{1}H NMR (acetone-*d*$_6$, 400 MHz, *δ* ppm): 3.84 (s, 12H, OCH$_3$); 6.97 (d, *J* = 8.4 Hz, 4H, H$_{9'}$); 7.01 (d, *J* = 8.4 Hz, 4H, H$_9$); 7.24 (d, *J* = 16.5 Hz, 2H, Hy′); 7.32 (d, *J* = 16.1 Hz, 2H, Hy); 7.51 (d, *J* = 5.5 Hz, 2H, H$_{5'}$); 7.60 (d, *J* = 8.4 Hz, 4H, H$_{8'}$); 7.66 (d, *J* = 8.7 Hz, 4H, H$_8$); 7.74 (d, *J* = 15.7 Hz, 2H, Hx′); 7.76 (d, *J* = 5.1 Hz, 2H, H$_5$); 7.78 (d, *J* = 16.5 Hz, 2H, Hx); 7.97 (d, *J* = 5.8 Hz, 2H, H$_{6'}$); 8.15(d, *J* = 5.8 Hz, 2H, H$_6$); 8.13 (dd, *J* = 5.1 Hz/8.4 Hz, 2H, Hc, Hc′); 8.72 (d, *J* = 8.8 Hz, 2H, Hd, Hd′); 8.74 (d, *J* = 5.1 Hz, 1H, Ha); 8.82 (d, *J* = 9.5 Hz, 1H, Ha′); 9.03 (s, 2H, H$_{3'}$); 9.06 (s, 2H, H$_3$); 9.28 (s, 1H, He); 9.78 (dd, *J* = 3.7 Hz/7.7 Hz, 2H, Hb, Hb′).

*2.6.5. [Ru(L-OCH$_3$)$_2$Aqphen](PF$_6$)$_2$ (**6**)*

Yield: 33%. *Anal.* Calc. for $RuC_{82}H_{60}N_8O_6P_2F_{12}$: C, 59.89; H, 3.68; N, 6.81. Found: C, 58.80; H, 3.63; N, 6.79%. IR (cm^{-1}): 3071 *ν*(CH aromatic); 2837 *ν*(CH aliphatic); 1671 *ν*(C═ O); 1596 *ν*(C═ N); 1254 *ν*(C—O—C asymmetric); 1027 *ν*(C—O—C symmetric); 842 and 557 *ν*(P—F$_6$). ^{1}H NMR (acetone-*d*$_6$, 400 MHz, *δ* ppm): 3.84 (d, *J* = 12.4 Hz, 12H, OCH$_3$); 6.97 (d, *J* = 8.6 Hz, 4H, H$_{9'}$); 7.02 (d, *J* = 8.5 Hz, 4H, H$_9$); 7.24 (d, *J* = 16.7 Hz, 2H, Hy′); 7.32 (d, *J* = 16.8 Hz, 2H, Hy); 7.53 (t, 2H, H$_{5'}$); 7.60 (d, *J* = 8.5 Hz, 4H, H$_{8'}$); 7.66 (d, *J* = 8.2 Hz, 4H, H$_8$); 7.74 (d, *J* = 15.7 Hz, 2H, Hx′); 7.76 (d, *J* = 5.1 Hz, 2H, H$_5$);7.79 (d, *J* = 15.4 Hz, 2H, Hx); 7.96 (d, *J* = 8.7 Hz, 1H, Hg); 7.99 (d, *J* = 9.6 Hz, 1H, Hg′); 8.02 (d, *J* = 5.9 Hz, 2H, H$_{6'}$); 8.13 (t, 1H, Hc); 8.16 (d, *J* = 6.3 Hz, 2H, H$_6$); 8.19 (t, 1H, Hc′); 8.27 (d, *J* = 7.5 Hz, 1H, Hf); 8.34 (d, *J* = 7.7 Hz, 1H, Hf′); 8.75 (d, *J* = 5.4 Hz, 2H, Hd, Hd′); 8.74 (d, *J* = 5.1 Hz, 2H, Ha, Ha′); 9.03 (s, 2H, H$_{3'}$); 9.06 (s, 2H, H$_3$); 9.28 (s, 1H, He);9.72 (d, *J* = 8.0 Hz, 1H, Hb); 9.79 (d, *J* = 7.7 Hz, 1H, Hb′).

3. Results and discussion

3.1. Synthesis and characterization

Each acceptor ligand (NN-A) was prepared according to the following literature procedures: Pyrazino[2,3-f][1,10]phenanthroline (ppl) [24], Dipyrido[2,3-a:2′,3′-c]phenazine (dppz) [25], 11-nitrodipyrido[2,3-a:2′,3′-c]phenazine (dppz-NO2) [26] and 10,11-[1,4-naphtalenedione]dipyrido[3,2-a:2′,3′-c]phenazine (Aqphen) [27].

Transition metal complexes *cis*-[Ru(L-OCH$_3$)$_2$(NN-A)](PF$_6$)$_2$: In general, all the complexes described in this work were prepared by reaction of the appropriate polypyridine ligand with the corresponding metal precursor *cis*-[Ru(L-OCH$_3$)$_2$Cl$_2$] as depicted in Scheme 2.

Characterization of the new products was achieved by means of IR, ^{1}H and COSY ^{1}H–^{1}H NMR spectroscopy and elemental analysis.

The solids of the new complexes were recrystallized from Me$_2$CO/Et$_2$O (1:1) and obtained as spectroscopically pure, air and thermally stable, red to dark-red microcrystalline solids in moderate yields (23%–51%).

The most remarkable common features observed in the IR spectra of these new compounds (**1**–**6**) were: (i) the existence of a sharp intense band at ca. 1249–1253 cm^{-1}, due to the asymmetric stretching vibration of the C—O—C group of the 4,4′-bis(2-(4-methoxyphenyl)styryl)-2,2′-bipyridine ligand, and a sharp medium intensity band at 1027 cm^{-1} due to the symmetric vibration of the C—O—C group; (ii) a very strong *ν*(PF$_6$) band at ca. 840–842 cm^{-1} and a sharp and strong *δ*(P—F) band at 557 cm^{-1}. Also, the IR spectra of compound **5** exhibited a strong band at 1511 cm^{-1} and a sharp medium intensity band at 1347 cm^{-1} attributed to the NO$_2$ group, whereas for complex **4** the C≡N stretching vibration appeared at 2227 cm^{-1} in the IR spectrum. Finally, compound **6** showed a sharp medium intensity band at 1671 cm^{-1} attributed to the *ν*(C═O) group, which is compatible with the presence of the naphthalenedione fragment.

Scheme 2. Synthesis of heteroleptic ruthenium complexes. NN-A = ppl, dppz-R; R: H, NO$_2$, CN, and Aqphen.

Table 1a
^{1}H NMR results for the free L-OCH$_3$ ligand, and for complexes (**1**–**6**).

Complex	OCH_3	H_3	$H_{3'}$	H_5	$H_{5'}$	H_6	$H_{6'}$	H_8	$H_{8'}$	H_9	$H_{9'}$	H_x	$H_{x'}$	H_y	$H_{y'}$
L-OCH$_3$	3.85	8.52		7.37		8.65		7.52		9.94		7.00		7.42	
1	3.84	9.00		7.66		8.02		7.66		7.00		7.76		7.30	
2	3.85	9.06	9.02	7.76	7.47	8.15	7.89	7.67	7.62	7.02	6.99	7.79	7.70	7.33	7.24
3	3.84	9.09	9.06	7.69	7.51	8.02	7.97	7.65	7.61	7.00	6.97	7.81	7.73	7.32	7.23
4	3.84	9.04	9.02	7.75	7.51	8.15	7.97	7.66	7.61	7.01	6.67	7.78	7.70	7.33	7.24
5	3.84	9.06	9.03	7.76	7.51	8.15	7.97	7.66	7.60	7.01	6.97	7.78	7.74	7.32	7.24
6	3.84	9.06	9.03	7.76	7.53	8.16	8.02	7.66	7.60	7.02	6.97	7.79	7.74	7.32	7.24

Table 1b
^{1}H NMR results for complexes (**2**–**6**) NN-A ligand.

Complex	H_a	$H_{a'}$	H_b	$H_{b'}$	H_c	$H_{c'}$	H_d	$H_{d'}$	H_e	H_f	$H_{f'}$	H_g	$H_{g'}$
2	9.36		9.66		8.13		8.71		–	–	–	–	–
3	8.46		9.74		8.13		8.67		8.18	–	–	–	–
4	8.03	8.37	9.76		8.17		8.73		8.66	–	–	–	–
5	8.74	8.82	9.78		8.13		8.72		9.28	–	–	–	–
6	8.74		9.72	9.79	8.13	8.19	8.75		9.28	8.27	8.34	7.96	7.99

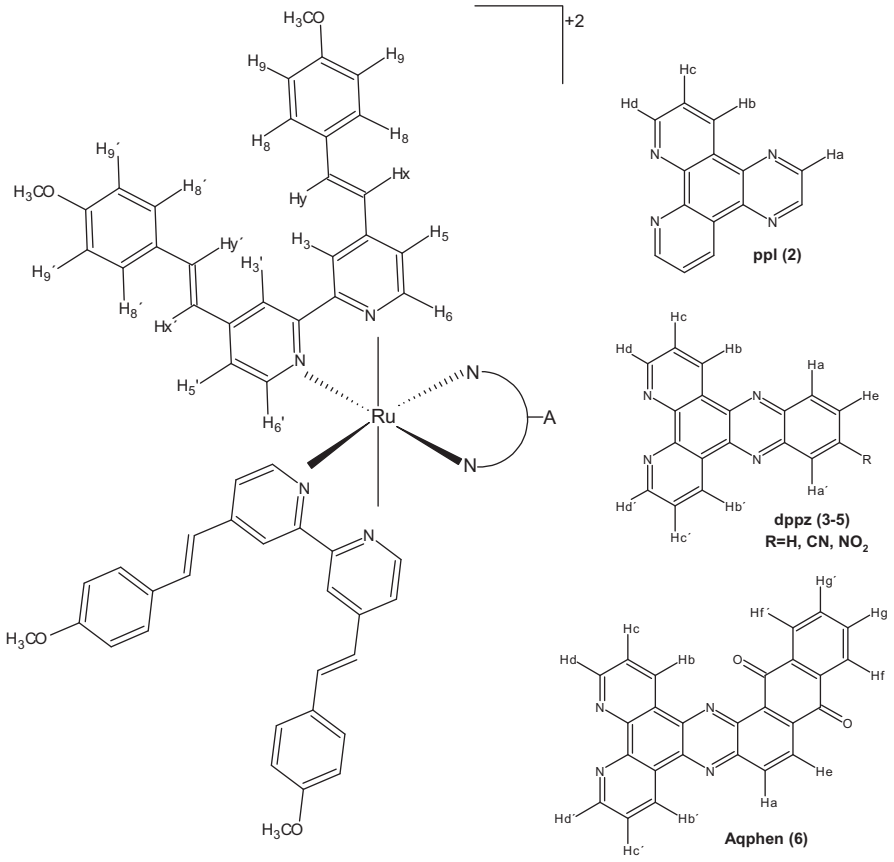

Fig. 3. Proton numbering for the ^{1}H NMR spectra of the complexes.

The ^{1}H NMR spectra are in agreement with the proposed structures of the complexes. These spectra are included as S1–S8 in Supplementary material. Tables 1a and 1b and Fig. 3 show the results and the assignments of the ^{1}H NMR signals. In comparison with the free ligands, the H_6, $H_{6'}$ protons as well as the H_d proton in ortho position with respect to the phenanthrolinic nitrogen atom in the NN-A ligand, appear at low field (around 8.72 ppm) as a consequence of their coordination to the metal.

Otherwise, the signal of the H_b proton of the NN-A ligand, the proton in *para* position to the pyrazine N of the acceptor ligand, appears at lower field (9.66–9.79 ppm). The shift in this signal, when compared with the corresponding free ligand, is fundamentally due to the anisotropic effect of the nitrogen atom in the pyrazine fragment. It can also be seen that the change in the signal position, although smooth, tends to vary with the acceptor strength of the ligand. As its strength increases, the electronic density around the proton of the phenanthroline fragment decreases and the signal shifts to lower fields.

With regard to the signals of the L-OCH$_3$ ligands, the expected and characteristic pattern can be observed: the doublet of the Hx

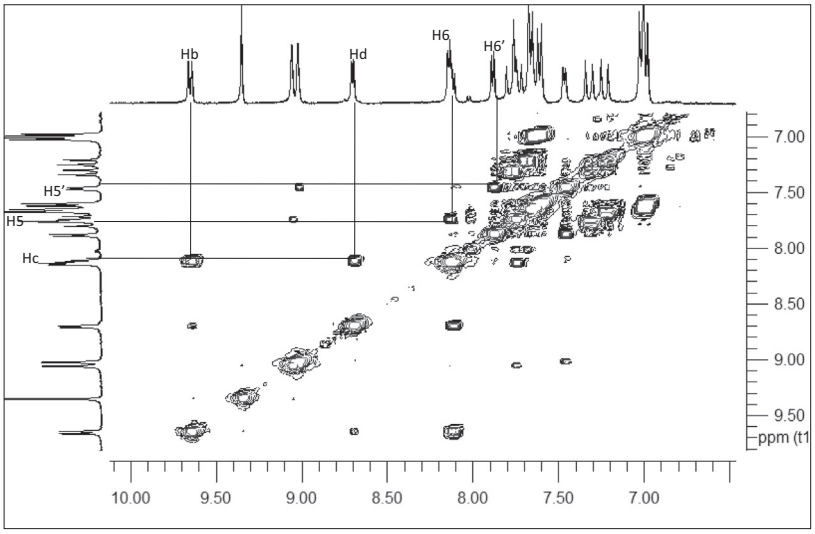

Fig. 4. COSY ^{1}H–^{1}H NMR spectrum of the [Ru(L-OCH_3)$_2$(ppl)]$(PF_6)_2$ complex.

Table 2
Oxidation potentials for complexes **1**–**6**.

Complex	Oxidation	
	$E_{1/2}$ Ru(II)/Ru(III) (V)	ΔE (mV)
[Ru(L-OCH_3)$_3$]$(PF_6)_2$(**1**)	1.06	116
[Ru(L-OCH_3)$_2$ppl]$(PF_6)_2$(**2**)	1.10	162
[Ru(L-OCH_3)$_2$dppz]$(PF_6)_2$(**3**)	1.13	98
[Ru(L-OCH_3)$_2$dppz-CN]$(PF_6)_2$(**4**)	1.16	153
[Ru(L-OCH_3)$_2$dppz-NO_2]$(PF_6)_2$(**5**)	1.12	94
[Ru(L-OCH_3)$_2$Aqphen]$(PF_6)_2$(**6**)	1.14	118

and Hy protons (7.23–7.81 ppm) is shifted by the presence of the electron density acceptor groups, and the signal of the donor group OCH_3 at around 3.84 ppm.

Finally, 2D-NMR spectra were registered for the new complexes in order to corroborate the assignments given above. Fig. 4 shows the spectrum for the [Ru(L-OCH_3)$_2$(ppl)]$(PF_6)_2$ complex. The correlations between some protons of the L-OCH_3 ligand, and of the NN-A ligand, are shown.

3.2. Cyclic voltammetry

Electrochemical data for complexes **1**–**6** were measured in acetonitrile solution; the data are compiled in Table 2. In the anodic region, the complexes exhibited quasi-reversible one-electron redox waves due to oxidation of the ruthenium metal. For all complexes the oxidation potential assigned to the $Ru^{III/II}$ couple was found at higher values than for the homoleptic complex as a consequence of increased back-bonding to the lower-lying π^* orbitals of the electron-acceptor ligands. The introduction of electron-withdrawing groups in dppz has little effect on the $Ru^{III/II}$ couple. This is because of the long distance from these groups to the metal center and the "blocking" effect of the pyrazine ring [26]. Nevertheless, an experimental tendency was observed for the acceptor character of the ligands: ppl < NO_2dppz < dppz < Aqphen < CNdppz.

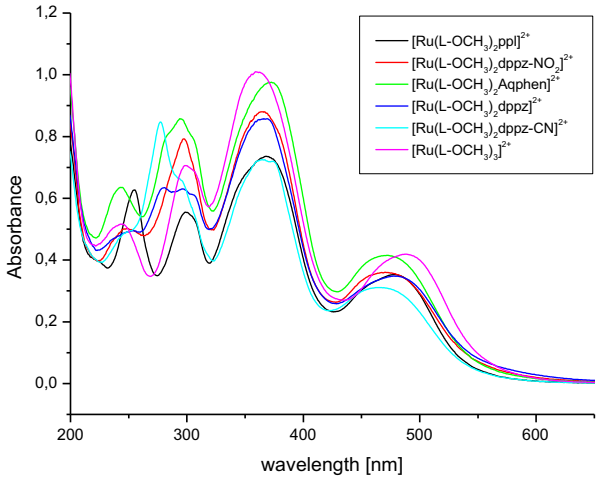

Fig. 5. Absorption spectra of complexes **1**–**6** in acetonitrile.

3.3. UV–Vis absorption spectra

The electronic absorption spectra of the Ru(II) complexes were measured in acetonitrile at room temperature, Table 3. In the UV

Table 3
Electronic absorption data for complexes **1**–**6**.

Complex	MLCT[#]	ILCT π–π^*	IL π–π^*/n–π^*
[Ru(L-OCH_3)$_3$]$(PF_6)_2$ (**1**)	488 (5.24)	359 (12.62)	296 (8.72)
[Ru(L-OCH_3)$_2$ppl]$(PF_6)_2$ (**2**)	479 (4.51)	368 (9.19)	299 (6.94)
[Ru(L-OCH_3)$_2$dppz]$(PF_6)_2$ (**3**)	475 (4.34)	369 (10.72)	281 (7.92)
[Ru(L-OCH_3)$_2$dppz-CN]$(PF_6)_2$ (**4**)	467 (3.89)	367 (9.06)	277 (10.59) sh 296
[Ru(L-OCH_3)$_2$dppz-NO_2]$(PF_6)_2$ (**5**)	470 (4.50)	365 (11.00)	298 (9.90)
[Ru(L-OCH_3)$_2$Aqphen]$(PF_6)_2$ (**6**)	472 (5.19)	372 (12.04)	294 (10.89)

[#] In CH_3CN at room temperature (ε 10^4 M^{-1} cm^{-1}).

region, three intense and sharp bands were observed corresponding to intra-ligand transitions (IL). The high-intensity absorption band around 350 nm can be ascribed mainly to a π–π^* IL transition, although some MLCT contribution should be considered [28–30].

In the visible range, complexes **1**–**6** exhibited very intense, broad Metal to Ligand Charge Transfer (MLCT) absorption bands, as is usually observed for related complexes [29] (see Fig. 5). In this case the same ILCT contribution may be present [26]. The lowest energy absorption maximum (488 nm, $\varepsilon = 5.24 * 10^4\ M^{-1}\ cm^{-1}$) was obtained for the homoleptic complex **1**, which contains only L-OCH_3 ligands, and that therefore can be taken as a "blank" or "reference". Considering (i) the position of the visible absorption band in the homoleptic complex **1**; (ii) that the presence of an acceptor group in the NN-A ligand shifts those bands to higher energy; and (iii) the intraligand bands are at higher energies, the MLCT is assigned as metal to the chromophoric ligand charge transfer, although overlapping MCLT transitions to L-OCH_3 and NN-A are most likely the reason for the broadening. The blue-shift in the MLCT bands is due to decreased electron density at Ru due to increased back-bonding to the acceptor ligands and to weak electronic coupling between the ruthenium and the low-lying π^* orbitals in the acceptor ligands.

3.4. Solvatochromic studies

Electronic absorption spectra for the new complexes were measured in different solvents, progressing from less polar to more polar: benzene, acetone, and acetonitrile; the values of the corresponding absorption maxima are recorded in Table 4. The UV–Vis spectra of solutions of **2**–**6** exhibit MLCT absorption in the 20 000–25 000 cm^{-1} range. For acetone, and acetonitrile, the effect of solvent polarity in the absorption maxima is small, although these maxima are ill-defined due to the broad nature of these bands. A similar behavior was observed in dichloromethane. The slight solvent dependence when comparing polar solvents can also be ascribed to overlapping MCLT transitions to L-OCH_3 and NN-A. In this context, the solvent discussion will be centered in comparing the more polar solvent, ACN, and the non-polar solvent, benzene. The 400–500 nm band shows negative solvatochromism [16], indicated by an hypsochromic shift of the absorption band when going from a less polar, benzene, to a more polar solvent, acetonitrile. This phenomenon is less marked for complex (**5**), that undergoes a small hypsochromic shift of 785 cm^{-1}, while for complexes (**2**, **3**, **4** and **6**) a noticeable blue shift in the MLCT band ($\Delta\lambda$ = 2138–2894 cm^{-1}) was noted.

The hypsochromic character of the solvent effect shows that the ground state is more polar and more stabilized in polar solvents than the MLCT excited state. This is in agreement with the assignment of the visible absorption band and electrochemical results. As seen from the first oxidation process, the HOMO orbital is centred on the metal, with a small change in its energy when the polypyridinic LL-A ligand changes.

Looking in particular to the solvent effect, a redistribution of the electronic density among the metal and the donor ligand is observed with a relatively low energy cost; in consequence a NLO response would be predicted. The magnitude of the electronic density redistribution, on passing from ground to excited state, seems to be influenced by the acceptor substituent in the R-dppz fragment in complexes. It is known that both, nitro and cyano groups have high electron acceptor character. Looking at the electrochemical results, the tendency indicates that in the ground state the cyano moiety is only slightly more acceptor than nitro, Nevertheless the solvent effect is clearly different when comparing the more polar solvent, ACN, and the non-polar solvent, benzene, pointing to nitro as a better acceptor.

In 2010, Le Bozec and co-workers [8] published theoretical results for beta values for M(II) complexes with 4,4′-bis(X-styryl)-2,2′bipyridine as *donor ligand*. When X is a nitro or cyano group, the visible band is assigned to ILCT and LLCT transitions, the $\lambda_{maximun}$ of the cyano substituted complex appearing at a slightly higher energy than the equivalent nitro complex. Theoretical calculations of the ground state dipolar moment give similar values for both, but when calculating the β_{SHG} parameter, a high value for X = nitro is observed, β_{SHG} (nitro) > β_{SHG} (cyano), independent of the elected functional used for the calculations. The results reported in the present work seem to be in agreement with Le Bozec results since complexes with different acceptor substituent groups have a different solvent effect. In our complexes, 4,4′-bis(X-styryl)-2,2′bipyridine is the donor moiety, with X = —OCH_3, while dppz-Y (with Y = cyano, nitro) is the *acceptor one*. As previously mentioned, Table 4, the MLCT band (visible region) was assigned as a MLCT to 4,4′-bis(X-styryl)-2,2′bipyridine. Taken into account that the visible band should also have a contribution from the MLCT to dppz-Y transition, and since both associated dipolar moments are vectorially in opposite directions, the NLO response should be related to a $\beta_{total} = |\beta\,(\text{MLCT donor})| - |\beta\,(\text{MLCT dppz-Y})|$. Considering a series of complexes, with the same donor ligand i (as is the case here reported), the β_{total} value should decrease as the acceptor character of the Y substituent increases, giving therefore a lesser solvent effect. According to this, for the complexes studied in this work, the results indicate that nitro (with a lesser solvent effect) is a better acceptor group in comparison with the cyano moiety.

A briefly consideration to the possibility of the presence of an ILCT in the chromophoric donor ligand must be done. In Le Bozec and co-workers paper, some complexes have Zn as metal center. In these complexes, no MLCT is possible. Associated to the ILCT band a rather high value of β_0 was measured [8]. Therefore it is not possible to discard completely a contribution of this transition to the visible absorption band in the complexes here reported.

If this would be the case, ILCT should reinforce the effect of the MLCT to dppz ligand. The solvent effect for the complexes with cyano and nitro substituents is different but, according to the discussion above, to define which is the variable responsible of such difference is not simple, when there are contribution of transitions with different vectorial directions.

Finally, considering the two state model expressions for beta, it can be seen that the variables that generate good values for the NLO parameter are, among others, high molar absorptivity and a large change in dipole moment between the ground and excited states ($\Delta\mu$). For the complexes reported here, the molar absorptivity is high, while $\Delta\mu$ is moderate. Therefore, a NLO response should be expected.

Table 4
Electronic absorption data for complexes **1**–**6** in different solvents.

Complexes	MLCT ACN cm^{-1}	MLCT Acetone cm^{-1}	MLCT Benzene cm^{-1}
$[Ru(L\text{-}OCH_3)_3](PF_6)_2$ (**1**)	20 492	20 492	–
$[Ru(L\text{-}OCH_3)_2ppl](PF_6)_2$ (**2**)	20 877	21 053	18 762
$[Ru(L\text{-}OCH_3)_2dppz](PF_6)_2$ (**3**)	21 053	20 833	18 519
$[Ru(L\text{-}OCH_3)_2dppz\text{-}CN](PF_6)_2$ (**4**)	21 413	21 053	18 519
$[Ru(L\text{-}OCH_3)_2dppz\text{-}NO_2](PF_6)_2$ (**5**)	21 277	21 186	20 492
$[Ru(L\text{-}OCH_3)_2Aqphen](PF_6)_2$ (**6**)	21 186	21 186	19 048

Acknowledgment

The authors thank Fondecyt Chile (Project Nos. 1070799 and 1110991), and Dr. Hubert Le Bozec and Javier Concepción for helpful discussions.

Appendix A. Supplementary data

Supplementary data associated with this article can be found, in the online version, at http://dx.doi.org/10.1016/j.poly.2014.09.004.

References

[1] H.S. Nalwa, Appl. Organomet. Chem. 5 (1991) 349.
[2] S.R. Marder, in: D.W. Bruce, D.O'. Hare (Eds.), Inorganic Materials, Wiley, New York, 1992, p. 116.
[3] N.J. Long, Angew. Chem., Int. Ed. Engl. 34 (1995) 21.
[4] I.R. Whittall, A.M. McDonagh, M.G. Humphrey, M. Samoc, Adv. Organomet. Chem. 42 (1998) 291.
[5] T. Fondum, K. Green, M. Randles, M. Cifuentes, A. Willis, A. Teshome, I. Asselberghs, K. Cáliz, M. Humphrey, J. Organomet. Chem. 693 (2008) 1605.
[6] G. Batema, M. Lutz, A. Spek, C. van Walree, C. Donegá, A. Meijerink, R. Havenith, J. Pérez-Moreno, K. Clays, M. Büchel, A. van Dijken, D. Bryce, G. van Klink, G. van Koten, Organometallics 27 (2008) 1690.
[7] P. Yuan, J. Yin, G. Yu, Q. Hu, S. Hua Liu, Organometallics 26 (2007) 196.
[8] A. Baccouche, B. Peigné, F. Ibersiene, D. Hammoutene, A. Boutarfaia, A. Boucekkine, C. Feuvrie, O. Maury, I. Ledouxand, H. Le Bozec, J. Phys. Chem. 114 (2010) 5429.
[9] L. Sanhueza, M. Barrera, I. Crivelli, Polyhedron 57 (2013) 94.
[10] A. Valente, S. Royer, M. Narendra, T. Silva, P. Mendes, M. Robalo, M. Abreu, J. Heck, M. Garcia, J. Organomet. Chem. 736 (2013) 42.
[11] E. Cariati, M. Pizzotti, D. Roberto, F. Tessore, R. Ugo, Coord. Chem. Rev. 250 (2006) 1210.
[12] S. Marder, C. Gorman, B. Tiemann, L. Cheng, J. Am. Chem. Soc. 115 (1993) 3006.
[13] S. Marder, L. Cheng, B. Tiemann, J. Chem. Soc., Chem. Commun. (1992) 672.
[14] M. Ruiz Delgado, J. Casado, V. Hernández, J. López Navarrete, J. Orduna, B. Villacampa, R. Alicante, J.-M. Raimundo, P. Blanchard, J. Roncali, J. Phys. Chem. C 112 (2008) 3109.
[15] N.-N. Ma, S.-L. Sun, C.-G. Liu, X.-X. Sun, Y.-Q. Qiu, J. Phys. Chem. A115 (2011) 13564.
[16] J. Heck, S. Dabek, T. Meyer-Friedrichsen, H. Wong, Coord. Chem. Rev. 190 (1999) 1217.
[17] H. Le Bozec, T. Renouard, Eur. J. Inorg. Chem. (2000) 229.
[18] S. Di Bella, Chem. Soc. Rev 30 (2001) 355.
[19] P. Wang, C. Klein, R. Humphry-Baker, S. Zakeeruddin, M. Gratzel, J. Am. Chem. Soc. 127 (2005) 808.
[20] K.-J. Jiang, N. Masaki, J. Xia, S. Noda, S. Yanagida, Chem. Commun. (2006) 2460.
[21] D. Martineau, M. Beley, P. Gros, S. Cazzanti, S. Caramori, C. Bignozzi, Inorg. Chem. 46 (2007) 2272.
[22] D. Kuang, S. Ito, B. Wenger, C. Klein, J.-E. Moser, R. Humphry-Baker, S. Zakeeruddin, M. Gratzel, J. Am. Chem. Soc. 128 (2006) 4146.
[23] A. Juris, S. Campagna, I. Bidd, I.-B. Lehn, R. Ziessel, Inorg. Chem. 27 (1988) 4007.
[24] A. Delgadillo, P. Romo, A. Leiva, B. Loeb, Helv. Chim. Acta 86 (2003) 2110.
[25] A. Edmond, H. Ahomsi, J.-C. Chambron, J.-P. Sauvage, J. Chem. Soc., Dalton Trans. (1990) 1841.
[26] A. Arancibia, J. Concepción, N. Daire, G. Leiva, A. Leiva, B. Loeb, R. del Río, R. Díaz, A. Francois, M. Valdivia, J. Coord. Chem. 54 (2001) 323.
[27] R. López, B. Loeb, T. Boussie, T. Meyer, Tetrahedron Lett. 37 (31) (1996) 5437.
[28] F. Gajardo, M. Barrera, R. Vargas, I. Crivelli, B. Loeb, Inorg. Chem. 50 (2011) 5910.
[29] A. Kleineweischede, J. Mattay, J. Organomet. Chem. 691 (2006) 1834.
[30] D. Martineau, M. Beley, P. Gros, J. Org. Chem. 71 (2006) 566.